Digest Journal of Nanomaterials and Biostructures Vol. 9, No. 4, October - December 2014, p. 1569 - 1578

INFLUENCE OF PREPARATION STEPS ON THE PROPERTIES OF ELECTROSPUN ZnO FIBERS

C. BUSUIOC*, A. EVANGHELIDIS, C. FLORICA, I. ENCULESCU
National Institute of Materials Physics, RO-077125, Magurele - Bucharest, Romania

ZnO nanofibers were obtained by calcination of electrospun $Zn(Ac)_2 \cdot 2H_2O$/PMMA composite fibers and characterized by X-ray diffraction, scanning electron microscopy and photoluminescence spectroscopy. The thermal treatment led to polymer burning and polycrystalline hexagonal ZnO phase formation. The average fiber diameters range between 450 and 600 nm before calcination and 200 - 300 nm after calcination. PL investigation revealed a strong dependence of ZnO fibers emission band on the calcination temperature. Furthermore, electrical contacts were fabricated by photolithography and electric characteristics were measured.

(Received October 20, 2014; Accepted December 1, 2014)

Keywords: ZnO, nanofibers, electrospinning, field effect transistors

1. Introduction

Zinc oxide (ZnO) represents a subject of choice for recent research regarding semiconductor materials with applications in electronics and optoelectronics, in areas where traditional materials, such as silicon, are becoming unsuited, increasingly expensive or difficult to process [1]. A direct band gap semiconductor (with Eg about 3.30 eV), ZnO has been proposed as the basis for a variety of optoelectronic applications [2], the bulk of which rely on its ease of processing and availability. Using wet chemical [3, 4], electrochemical [5, 6] or physical [7, 8] methods, or combinations thereof, geometries ranging from thin films to complex shaped nanoparticles can be obtained, offering a great degree of control and scalability. Polymorphism is a main characteristic of ZnO nanostructures and can be further exploited for interesting applications.

Another field of study which has gained popularity over the last few decades is electrospinning [9]. This process can produce continuous, uniform, sub-micrometer diameter fibers by using a relatively simple experimental setup and inexpensive supplies. In its most basic form, a droplet of polymer solution at the tip of a spinarette, e.g. a syringe needle or a pipette, is charged in a high electric field, causing its deformation into a cone. Further, from the cone's tip a polymer solution jet is ejected and collected as a polymer fiber on an electrode opposing the needle. By continually supplying solution to the spinarette, the process can be carried out over long periods of time, yielding large amounts of nanofibers in the form of a nonwoven mesh.

A two-step process is employed for fabricating in this manner inorganic fibers such as oxides. After performing electrospinning from a solution containing both a carrier polymer and a metal salt, annealing was employed for removing the organic component, the process leading to the formation of the corresponding metal oxide component. Numerous results were reported on ZnO fibers obtained through an electrospinning approach using different polymers such as polyvinyl alcohol [10-13], polyvinyl acetate [14-16], polyvinylpyrrolidone [17-19], cellulose acetate [20] or polyacrylonitrile [21] as carriers. Various solvents were employed ranging from water to N,N-dimethylformamide [18, 19]. It was shown that the diameter of the precursor fibers is a function of the concentration of zinc salts, while the morphology of ZnO fibers is influenced by the calcination/annealing time [10]. P. Singh *et al.* [21] demonstrated the efficacy of mesoporous

*Corresponding author: cristina.busuioc@infim.ro

ZnO nanofiber mats obtained by electrospinning in wastewater treatment, while S. Wei *et al.* [19] reported on the ethanol sensing properties of electrospun ZnO fibers. Wei *et al.* [18] synthesized solid and hollow ZnO fibers by single capillary electrospinning.

H. Wu *et al.* [14] evidenced a field-effect transistor behavior in electrospun single ZnO nanofiber, which shows that pure ZnO nanofiber is an intrinsic n-type semiconductor. Park *et al.* [15] reported that the calcination atmosphere has a small influence on the electrical transport properties of electrospun ZnO nanofibers, while the grain boundaries found in each ZnO nanofiber act as barriers for electron flow.

In this work, we have used the electrospinning technique to obtain ZnO fibers from polymer solutions containing a varying amount of $Zn(Ac)_2 \cdot 2H_2O$. The resulting fibers were subjected to thermal treatment at different temperatures, which led to ZnO crystallization, as well as diameter reduction. The influence of $Zn(Ac)_2 \cdot 2H_2O$ concentration and calcination temperature on ZnO fibers properties were discussed. Further, a simple photolithographical process was employed to contact such semiconducting fibers placed on silicon substrates. The influence of a bottom gate, i.e. the n++ silicon substrate on the transport properties of the fibers was determined.

2. Experimental part

To fabricate zinc oxide (ZnO) fibers, zinc acetate dihydrate ($Zn(Ac)_2 \cdot 2H_2O$, Sigma-Aldrich, ≥98%) and polymethyl methacrylate (PMMA, MW = 350.000, Sigma-Aldrich) were used as starting materials, with N,N-dimethylformamide (DMF, ≥99,8%, Sigma-Aldrich) as solvent. The electrospinning solutions were obtained by mixing equal volumes of precursor solutions: $Zn(Ac)_2 \cdot 2H_2O$/DMF and PMMA/DMF. The concentration of $Zn(Ac)_2 \cdot 2H_2O$ in the final solution was varied (2, 5 or 7.5 wt.%), while the concentration of PMMA was set to 5 wt.%. Further, the $Zn(Ac)_2 \cdot 2H_2O$/PMMA/DMF solution was loaded in a plastic syringe with a blunt tipped stainless needle, which was attached to a syringe pump. The solution feeding rate was adjusted to 0.5 mL/h and a positive voltage of 15 kV was applied to the needle. Silicon plates were employed as collector substrates, being placed at a distance of 15 cm from the tip of the needle. In order to obtain single phase crystalline ZnO fibers, the electrospun fibers were then calcined in a convection oven for 8 h at 450, 600 or 800 °C, in air. The thermal treatment enabled polymer burning, acetate decomposition and ZnO formation.

The ZnO fibers were investigated by X-ray diffraction (XRD), scanning electron microscopy (SEM) and photoluminescence spectroscopy (PL). A Bruker D8 ADVANCE diffractometer with Ni filtered Cu-Kα radiation (λ = 0.154 nm), 2θ ranging between 20 and 60 °, was used to identify the crystalline phases and the structure of the calcined fibers. The microstructure of precursor and ZnO fibers was analyzed with an Evo 50 XVP scanning electron microscope. The photoluminescence spectra were recorded with a FL 920 Edinburgh Instruments spectrometer.

In order to study the electrical properties of ZnO fibers and to explore the possibility of developing an application, further processing of the samples was required. A small amount of precursor fibers were deposited on SiO_2/Si substrates and calcined at the aforementioned temperatures. Using photolithography, a conventional lithographic technique, interdigitated contacts were placed onto the calcined fibers. The quantity of fibers present on the substrates demanded special attention, in order to avoid shortcircuits due to possible errors within the lift-off process. The metals used for contacting were Ti (100 nm) and Au (300 nm), which were deposited by sputtering and thermal vacuum evaporation, respectively. The contacts have a width of about 4 μm, with a gap of 4 μm in between. The electrical characteristics were determined using a Keithley 4200 SCS and a Cascade Microtech MPS 150 probe station.

3. Results and discussion

The phase composition and crystal structure of ZnO fibers were examined by XRD. Fig. 1 displays the X-ray diffractograms of ZnO fibers prepared from 5 wt.%. $Zn(Ac)_2 \cdot 2H_2O$ solution

and calcined at different temperatures. The diffraction peaks placed at 2θ: 31.7, 34.4, 36.2, 47.5, 56.6, corresponding to (100), (002), (101), (102), (110) Miller indices, reveal the formation of hexagonal wurtzite ZnO phase (JCPDS 36-1451). The supplementary diffraction peaks are attributed to the substrate. The samples present high crystallinity and average crystallite sizes of 42 nm (450 °C), 59 nm (600 °C) and 66 nm (800 °C), respectively. It is obvious that the increase of the calcination temperature leads to larger ZnO crystallites. The average crystallite size (D) was estimated from the full width at half maximum (FWHM) of the (101) diffraction peak by using the Scherrer equation: $D=K\cdot\lambda/(\beta\cdot\cos\theta)$, where K is a dimensionless shape factor with a typical value of about 0.9, λ is the X-ray wavelength (0.154nm), β is the FWHM value and θ is the Bragg angle. All prepared samples exhibit similar crystallinity characteristics.

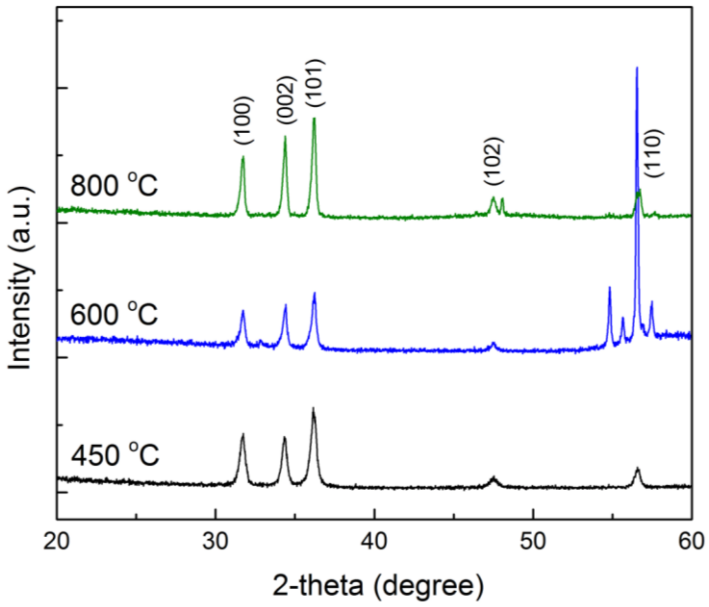

Fig. 1. XRD patterns of ZnO fibers prepared from 5 wt.%. $Zn(Ac)_2\cdot 2H_2O$ solution and calcined at different temperatures.

The evolution of fiber morphology was investigated by SEM. The addition of $Zn(Ac)_2\cdot 2H_2O$ to the precursor solution changes its response to the electric field, such that the resulting fibers are of smaller diameter than those produced from a polymer solution. However, the variation of $Zn(Ac)_2\cdot 2H_2O$ concentration (from 2 to 7.5 wt.%) does not lead to a noticeable change in fiber size. The fibers obtained by electrospinning a precursor solution containing 7.5 wt.% $Zn(Ac)_2\cdot 2H_2O$ are smooth, continuous and exhibit an average diameter of about 500 nm (Fig. 2 (a and a')). The thermal treatment further reduces the fiber diameter, to around 250 nm, but also modifies the overall aspect of the non-woven mats, which became discontinuous, most likely due to the contraction caused by the burning of the polymer matrix. Moreover, in the case of using a 2 or 5 wt.% $Zn(Ac)_2\cdot 2H_2O$ precursor solution, the calcined fibers have the tendency to break and form disparate particles (Fig. 2 (b and b') and (c and c')), a phenomenon that is caused by the Rayleigh instability [22].

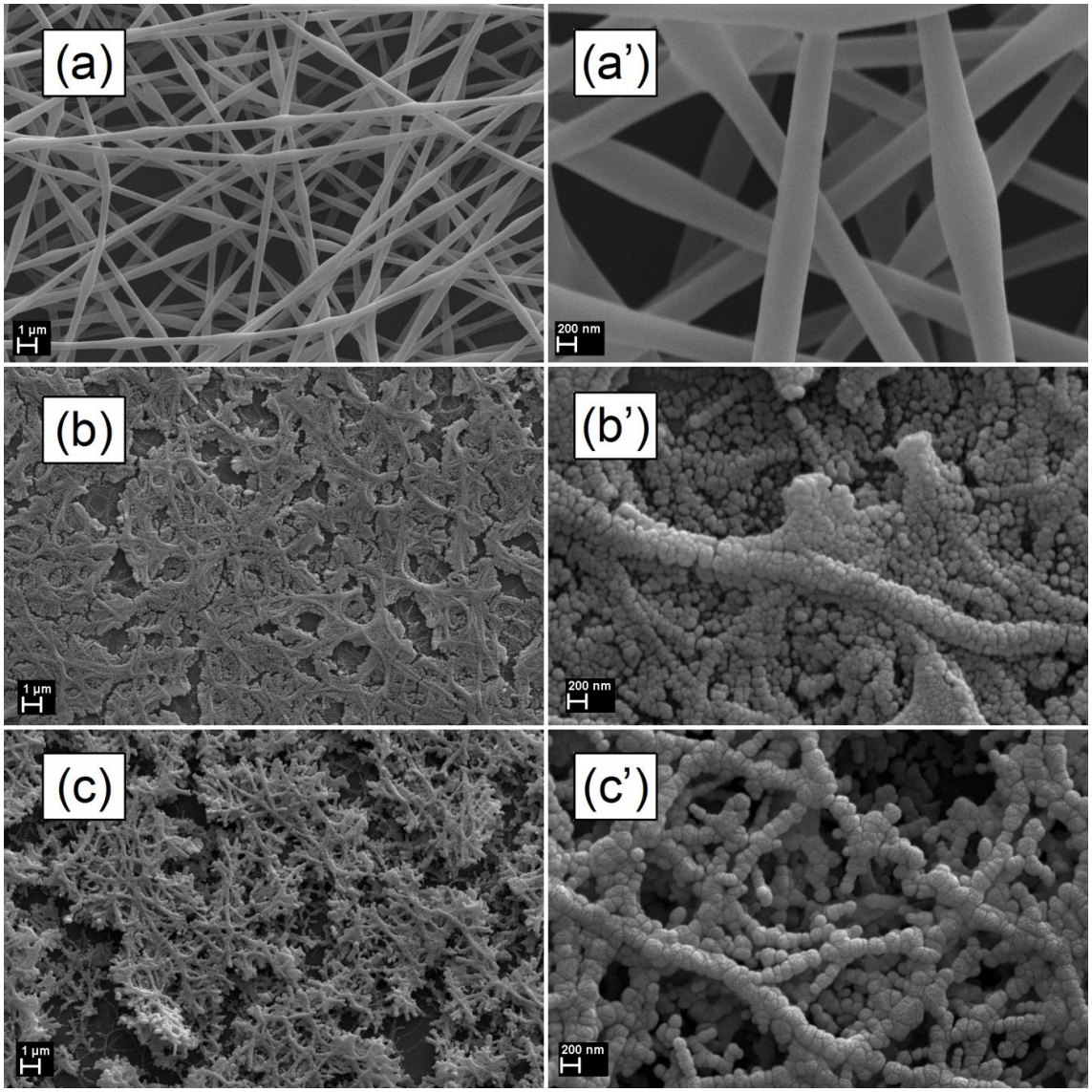

Fig. 2. SEM images of the precursor fibers (a and a') ZnO fibers prepared from 2 wt.% (b and b') and 5 wt.% (c and c') $Zn(Ac)_2 \cdot 2H_2O$ solution and calcined at 800 °C.

It can be concluded that an insufficient content of Zn^{2+} in the electrospinning solution leads to the formation of discontinuous ZnO fibers or even ZnO particles. As well, the crystallites size and the apparent quality of individual fibers increase with the calcination temperature. The samples treated at 450 °C present fibers interconnected by membranes as aggregates of ZnO crystallites (Fig. 3 (a and a')). At 600 and 800 °C (Figs. 3 (b and b') and (c and c')) the membranes disappear and the crystallites join in larger grains which represent the segments of individual ZnO fibers.

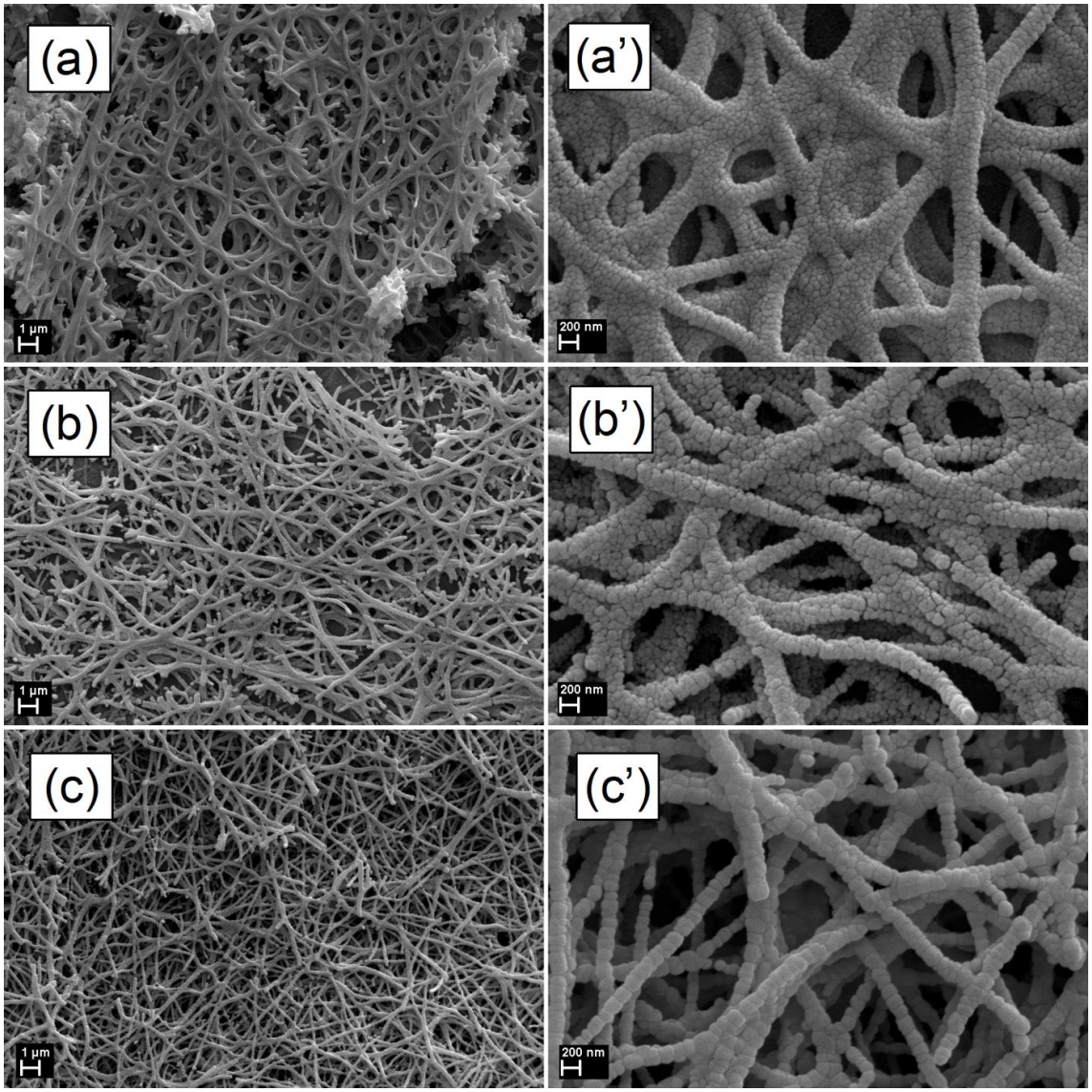

Fig. 3. SEM images of ZnO fibers prepared from 7.5 wt.% $Zn(Ac)_2 \cdot 2H_2O$ solution and calcined at 450 °C (a and a'), 600 °C (b and b') and 800 °C (c and c')

The optical properties of the ZnO fibers were also investigated, Fig. 4a presenting the optical reflection spectra of five different samples. The band-to-band transition in ZnO is evidenced by the pronounced decrease of reflectance below 400 nm. Using the reflectance data, ($F(R)$) was calculated and the $[F(R) \cdot E]^{1/2}$ function was plotted versus photon energy (E) in order to estimate the band gap values (Fig. 4b). The Kubelka-Munk function, expressed as $F(R)=(1-R)^2/(2 \cdot R)$, where R is the observed diffuse reflectance. The resulting band gap values are 3.19 eV±0.02 eV, which is in good agreement with previously reported data [20, 23] and prove that the processing conditions do not affect the optical properties of ZnO fibers.

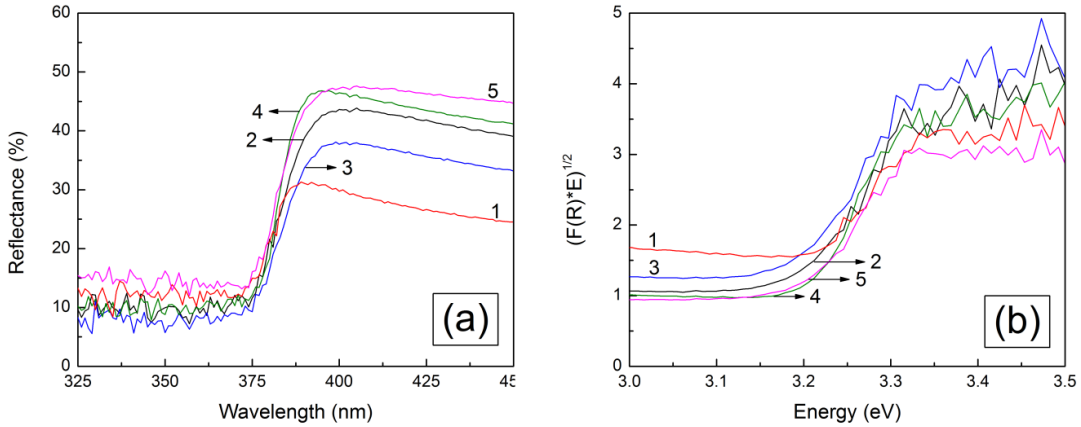

Fig. 4. Reflectance spectra (a) and representation of Kubelka-Munk function employed to estimate the band gap values of ZnO fibers prepared from: 2 wt.%. $Zn(Ac)_2 \cdot 2H_2O$ solution and calcined at 800 °C (curve 1), 5 wt.%. $Zn(Ac)_2 \cdot 2H_2O$ solution and calcined at 450 °C (curve 2), 600 °C (curve 3) or 800 °C (curve 4) and 7.5 wt.%. $Zn(Ac)_2 \cdot 2H_2O$ solution and calcined at 800 °C (curve 5)

Further, the photoluminescence properties of ZnO fibers were studied, since ZnO is a promising material in the field of optoelectronic devices. It is well known that ZnO light emission is either due to near band to band recombination (excitonic peak) or related to point defects such as zinc or oxygen vacancies or interstitials [23]. Fig. 5 shows the emission spectra of ZnO fibers prepared from a 5 wt.%. $Zn(Ac)_2 \cdot 2H_2O$ solution and calcined at 3 different temperatures. In our case, the excitonic peak appears for all calcination temperatures, being centered at approximately 380 nm. This behavior indicates that high quality ZnO fibers can be reliably obtained by electrospinning a Zn^{2+} containing polymer solution. Moreover, the PL spectrum of the sample calcined at 800 °C exhibits a strong and broad emission peak with maximum at approximately 515 nm, which corresponds to a high concentration of oxygen interstitials. In the case of the sample thermally treated at 600 °C, the defect related emission peak is wider and shifted to the right (centered at approximately 620 nm), being attributed to O vacancies or Zn interstitials. It is obvious that the photoluminescence peak intensity increases as the calcination temperatures and average crystallite size increase, which can be seen for all fabricated samples.

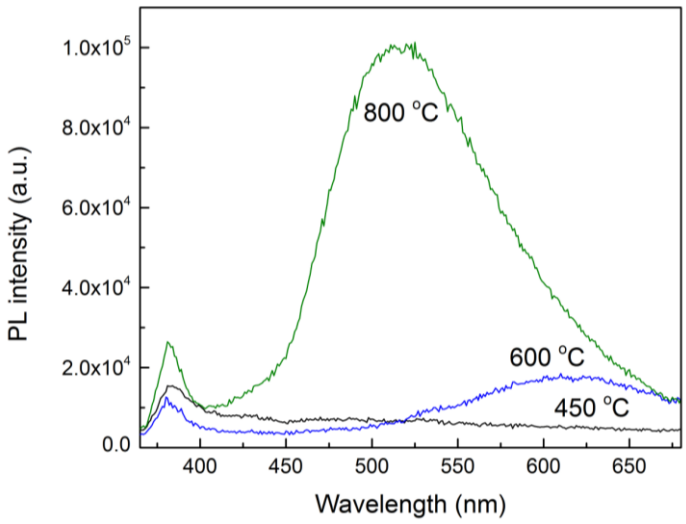

Fig. 5. PL spectra of ZnO fibers prepared from 5 wt.%. $Zn(Ac)_2 \cdot 2H_2O$ solution and calcined at different temperatures

The electrical properties of ZnO nanofibers were investigated after performing the photolithography process and depositing a Ti (100 nm) / Au (300 nm) layer as contacts. The digits have a width of about 4 μm, with a 4 μm gap (Fig. 6).

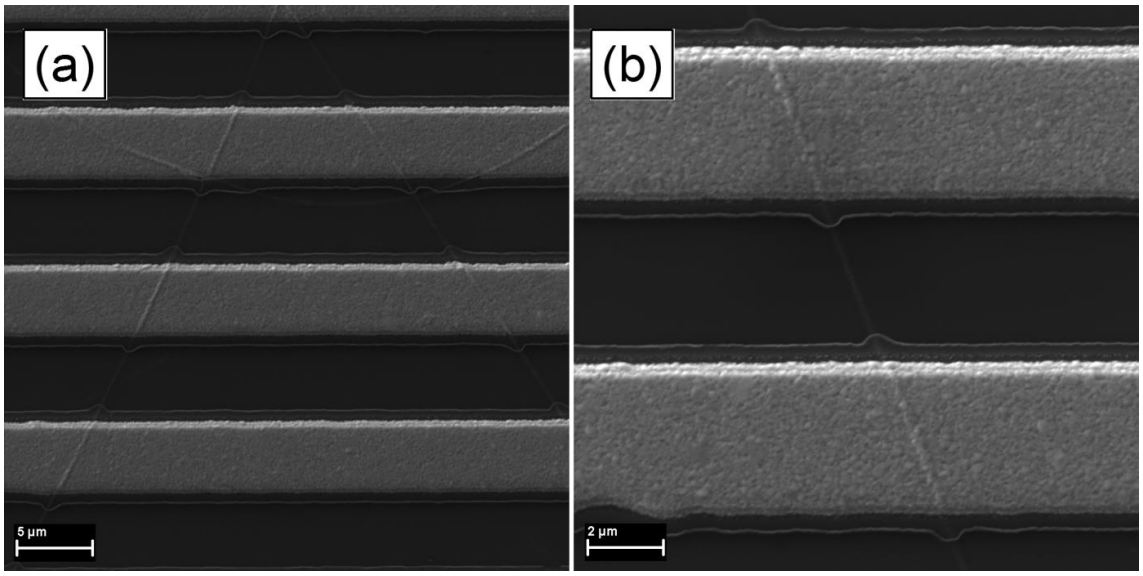

Fig. 6. SEM images of the interdigitated electrodes deposited onto ZnO nanofibers to provide electrical measurements

The current-voltage characteristics were measured for the electrospun ZnO nanofibers prepared from 7.5 wt.% $Zn(Ac)_2 \cdot 2H_2O$ solution, deposited onto SiO_2/Si substrate and calcined at 800 °C (Fig. 7). The I-V curve measured after the deposition of Ti/Au contacts, at room temperature, shows a back-to-back Schottky diode characteristic (Fig. 7b), which changes to a quasi-ohmic one after annealing at 350 °C (Fig. 7c). By performing the thermal treatment, the height of the potential barrier decreases due to the introduction of metal atoms into the semiconductor lattice.

When exposed to the ambient atmosphere, oxygen species are adsorbed on the nanofibers surface. These species form O_2^{2-}, O_2^-, O^{2-} ions after trapping electrons from the conductance band, leading to a space charged layer on the surface of the material [24]. Because electrons are extracted from the conductance band, the surface potential barrier becomes higher and thus the resistance is high [25, 26].

If the surface is passivated with a PMMA thin layer, an increase with a factor of 20 in the current can be observed (Fig. 7d).

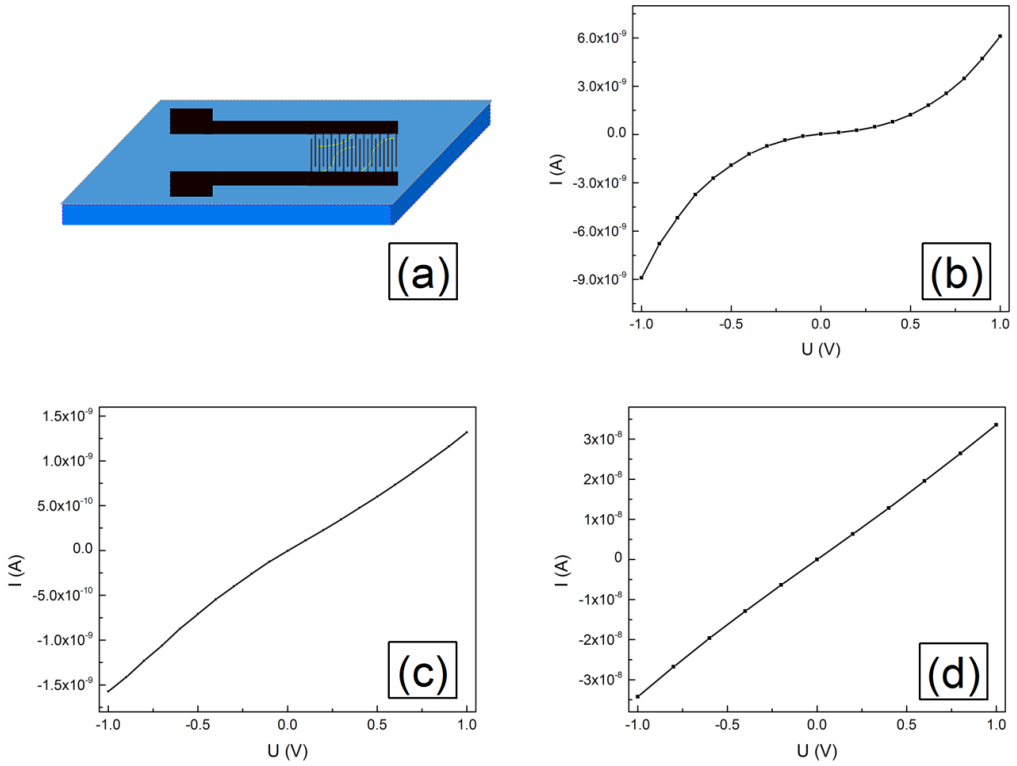

Fig. 7. (a) Schematic view of the system of contacting nanofibers; (b) current-voltage characteristics for as-deposited ZnO nanofibers with Ti/Au electrodes: annealed at 350 °C and (c) annealed at 350 °C and passivated with a thin layer of PMMA (d).

To fabricate a back gated field effect transistor, a contact was placed on the n++ doped Si as well. The thickness of the SiO_2 dielectric layer was about 50 nm. The family of output characteristics for the ZnO nanofiber based field effect transistor was then measured by sweeping the source-drain voltage from -1 V to 7 V and applying a back gate voltage ranging from -3V to 9V, with a step of 3V (Fig. 8). These source-drain characteristics are typical for an n-channel field effect transistor, where the conductance in the channel is increased by injecting carriers with the applied gate voltage.

By passivating the surface with a PMMA thin layer, an increase with a factor of 3 in the current is observed for the same applied voltages, at the same values of the gate voltages (Fig. 8b).

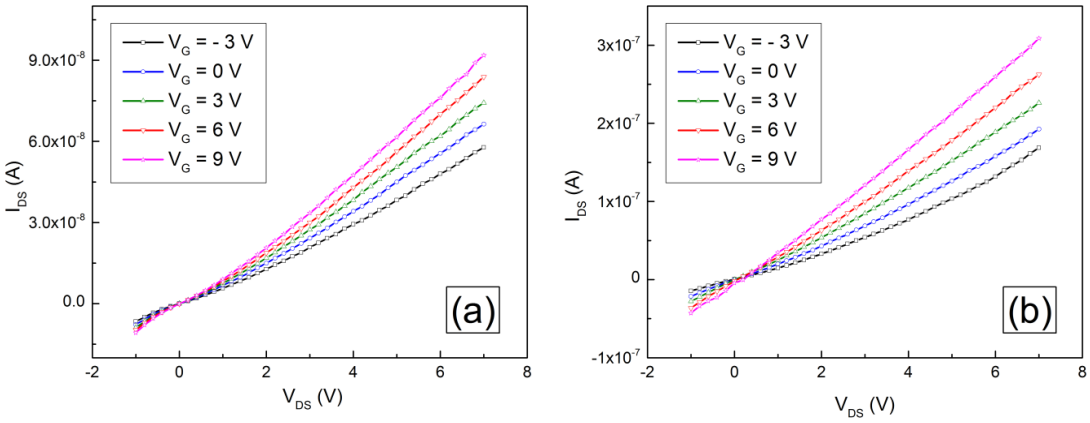

Fig. 8. Output characteristics of a ZnO nanofiber based field effect transistor measured while the channel was not passivated (a) and while covered with a thin layer of PMMA (b).

4. Conclusions

ZnO nanofibers were successfully prepared using electrospinning from a solution containing PMMA and followed by calcination at different temperatures. The thermal treatment leads to hexagonal wurtzite ZnO phase formation and fiber diameter reduction. The morphology of the resulting fibers is strongly influenced by the concentration of $Zn(Ac)_2 \cdot 2H_2O$ in the precursor solution, as well as by the thermal treatment temperature. The photoluminescence investigation evidenced the evolution of point defects with increasing calcination temperature. All samples exhibit band gap values of 3.19 eV±0.02 eV determined by reflectance spectra.

By providing the nanofibers with electrical contacts by photolithography and fabricating a back gate field effect transistor structure with the ZnO nanofiber as channel, a strong dependence with the applied gate voltage was observed. An increase in the drain-source current is induced when passivating the surface, which improves the electrical properties of the transistor. Such thin semiconducting fibers prepared by a straightforward approach can be easily employed as building blocks for bio or chemical sensors.

Acknowledgments

The authors gratefully acknowledge the financial support of UEFISCDI (project 159/2012 HEFFES). The author Cristina Busuioc acknowledges the Sectoral Operational Programme Human Resources Development 2007-2013 of the Ministry of European Funds (Financial Agreement POSDRU/159/1.5/S/132397).

References

[1] F. Rahman, Nanostructures in Electronics and Photonics, Pan Stanford Publishing, Singapore (2008).
[2] N.H. Nickel, E. Terukov, Zinc Oxide - A Material for Micro- and Optoelectronic Applications, Spinger (2005).
[3] N. Preda, M. Enculescu, C. Florica, A. Costas, A. Evanghelidis, E. Matei, I. Enculescu, Dig. J. Nanomater. Biostruct. **8**, 1591 (2013).
[4] T.H. Lee, H. Ryu, W.J. Lee, J. Alloy. Compd. **597**, 85 (2014).
[5] E. Matei, M. Enculescu, N. Preda, I. Enculescu, Mater. Chem. Phys. **134**, 988 (2012).
[6] N.K. Hassana, M.R. Hashima, J. Alloy. Compd. **577**, 491 (2013).
[7] W. Gao, Z. Li, Ceram. Int. **30**, 1155 (2004).
[8] S. Thanka Rajan, B. Subramanian, A.K. Nanda Kumar, M. Jayachandran, M.S. Ramachandra Rao, J. Alloy. Compd. **584**, 611 (2014).
[9] S. Ramakrishna, K. Fujihara, W.E. Teo, T.C. Lim, Z. Ma, An Introduction to Electrospinning and Nanofibers, World Scientific Publishing, Singapore (2005).
[10] H. Wu, W. Pan, J. Am. Ceram. Soc. **89**, 699 (2006).
[11] W. Wang, H. Huang, Z. Li, H. Zhang, Y. Wang, W. Zheng, C. Wang, J. Am. Ceram. Soc. **91**, 3817 (2008).
[12] H. Ren, Y. Ding, Y. Jiang, F. Xu, Z. Long, P. Zhang, J. Sol-Gel Sci. Technol. **52**, 287 (2009).
[13] M. Zhao, X. Wang, L. Ning, H. He, J. Jia, L. Zhang, X. Li, J. Alloy. Compd. **507**, 97 (2010).
[14] H. Wu, D. Lin, R. Zhang, W. Pan, J. Am. Ceram. Soc. **91**, 656 (2008).
[15] J.Y. Park, J.J. Kim, S.S. Kim, Microelectron. Eng. **101**, 8 (2013).
[16] S. Yun, S. Lim, J. Solid State Chem. **184**, 273 (2011).
[17] D. Lin, H. Wu, R. Zhang, W. Pan, Chem. Mat. **21**, 3479 (2009).
[18] S. Wei, M. Zhou, W. Du, Sens. Actuator B-Chem. **160**, 753 (2011).
[19] S. Wei, S. Wang, Y. Zhang, M. Zhou, Sens. Actuator B-Chem. **192**, 480 (2014).
[20] R. Liu, Y. Huang, A. Xiao, H. Liu, J. Alloy. Compd. **503**, 103 (2010).
[21] P. Singh, K. Mondal, A. Sharma, J. Colloid Interface Sci. **394**, 208 (2013).
[22] P.W. Fan, W.L. Chen, T.H. Lee, Y.J. Chiu, J.T. Chen, Macromolecules **45**, 5816 (2012).

[23] E. Matei, I. Enculescu, Mater. Res. Bull. **46**, 2147 (2011).
[24] P. Rai, Y.S. Kim, H.M. Song, M.K. Song, Y.T. Yu, Sens. Actuator B-Chem. **165**, 133 (2012).
[25] N. Yamazoe, Sens. Actuator B-Chem. **5**, 7 (1991).
[26] J. Xu, J. Han, Y. Zhang, Y. Sun, B. Xie, Sens. Actuator B-Chem. **132**, 334 (2008).
[27] W.K. Hong, B.J. Kim, T.W. Kim, G. Jo, S. Song, S.S. Kwon, A. Yoon, E.A. Stach, T. Lee, Colloid Surf. A-Physicochem. Eng. Asp. **313–314**, 378 (2008).